Natural Convection of a Paramagnetic Liquid Controlled by Magnetization Force

Syou Maki and Mitsuo Ataka
National Institute of Advanced Industrial Science and Technology (AIST), Ikeda, 563-8577, Japan

Toshio Tagawa and Hiroyuki Ozoe
Institute for Materials Chemistry and Engineering, Kyushu University, Kasuga, 816-8580, Japan

Wasuke Mori
Faculty of Science, Kanagawa University, Hiratsuka, 259-1293, Japan

DOI 10.1002/aic.10460
Published online March 1, 2005 in Wiley InterScience (www.interscience.wiley.com).

Rayleigh–Benard natural convection of aqueous gadolinium nitrate solution (paramagnetic) was studied experimentally and numerically in the presence of upward magnetization force in a framework similar to that proposed by Braithwaite et al. With the magnetic susceptibility of the gadolinium nitrate solution reevaluated by the Gouy method, the measured heat transfer rates were found to agree with Silveston's experimental curve, which represents the relationship between the Nusselt number (Nu) and the magnetic Rayleigh number (Ra_m). Furthermore, three-dimensional numerical computations were also carried out. Every convection flow pattern became axisymmetric, and the computed Nu agreed with Silveston's curve when Ra_m was used in place of the Rayleigh number.
 AIChE J, 51: 1096–1103, 2005
Keywords: magnetization force, convection, gadolinium nitrate, paramagnetic liquid, magnetic susceptibility

Introduction

Braithwaite et al.[1] measured the heat transfer rates of natural convection of gadolinium nitrate solution (paramagnetic liquid) in a bore space of a superconducting magnet and found that the heat transfer rates can be enhanced or suppressed, depending on the direction of magnetization force that a strong magnetic field generates. They proposed the magnetic Rayleigh number (Ra_m) with which the average heat transfer rates [Nusselt number (Nu)] can be correlated in a single curve over the graph of Nu vs. Ra_m. Following their report, Maki et al.[2] studied the same problem with air and found the average heat transfer rates can be correlated well with the magnetic Rayleigh number. They also found that their experimental and numerical heat transfer rates agree with Silveston's experimental curve.[3] However, on replotting the experimental data by Braithwaite et al. on their graph of Nu vs. Ra_m, they found that the latter data differ from Silveston's curve. Control of convection with the magnetization force is an important engineering problem in achieving effective heat transfer. In addition, Maki et al.[4] recently succeeded in growing protein crystals in a floating state by using magneto-Archimedes effect[5,6] in a paramagnetic aqueous gadolinium chloride solution, leading to improved crystalline quality. The quality improvement may arise from levitation or from modified convection, which constitutes the motivation of the present work. We used the aqueous gadolinium nitrate solution as Braithwaite et al.[1] did and obtained the results reported in this communication.

Correspondence concerning this article should be addressed to M. Ataka at m-ataka@aist.go.jp.

Table 1. Concentration, Density, and Magnetic Susceptibility of the Solution (at 298 K)*

	c_{Gd} (mol/kg)	ρ_{sol} (kg/m^3)	$\chi \times 10^7$ (m^3/kg)	$\chi_m \times 10^5$
Exp. data 1	0.0715	1020	0.139	1.42
	0.148	1044	0.407	4.25
	0.218	1063	0.636	6.76
Exp. data 2	0.0198	1001	−0.0267	−0.267
	0.0497	1010	0.0698	0.705
	0.1000	1025	0.230	2.36
	0.2001	1057	0.558	5.90
	0.4001	1125	1.22	13.7
	0.7003	1236	2.17	26.8
	0.9987	1377	3.13	43.1

*c_{Gd} is the concentration of gadolinium nitrate (mol/kg), ρ_{sol} is the density of the solution, χ is the magnetic susceptibility of the solution (m^3/kg), and χ_m is the nondimensional magnetic susceptibility of the solution, $\chi_m = \rho_{sol}\chi$.

Measurement of the Magnetic Susceptibility of $Gd(NO_3)_3$ Solution

The magnetic susceptibility of gadolinium nitrate hexahydrate was evaluated by the Gouy method at 298 K. The measurement was carried out two times. Table 1 shows the measured concentration, density, and magnetic susceptibility of ten solutions. Because magnetic susceptibility of paramagnetic materials is temperature dependent, all the results were converted by using Curie's law in comparison with the results by Braithwaite et al. at 288 K (15°C)[1] (we presume their room temperature as 288 K hereafter).

Figure 1 shows the relationship between the magnetic susceptibilities and the concentrations of gadolinium nitrate, and the filled circles (Exp. data 1) and the filled triangles (Exp. data 2) represent the results converted at 288 K. Figure 1A shows the measured results in the proximity of the experimentally used concentration of 0.148 mol/kg (see below). It is shown that the data points fall on a straight line. The open diamond represents the diamagnetic susceptibility of pure water. This literature value is also on the straight line. Figure 1B represents the whole area of measurements, and also includes the data given by Braithwaite et al.[1] In their report, however, the concentration of the gadolinium ions cannot be known exactly because $Gd(NO_3)_3$ can be anhydrate, pentahydrate, and hexahydrate. The three possibilities are included in Figure 1B; if their solution was the anhydrate, pentahydrate, or hexahydrate, the values correspond to the open square (a), the open triangle (b), and the open circle (c), respectively. From the results, it is found that the magnetic susceptibility comes closer to our results if the solution was prepared with pentahydrate or hexahydrate.

Experimental

The heat transfer rates of natural convection of aqueous gadolinium nitrate solution were measured in a shallow cylindrical enclosure (a) in Figure 2 heated from below and cooled from above. The concentration of gadolinium nitrate used was $c_{Gd} = 0.148$ mol/kg, and its density $\rho_{sol} = 1044$ kg/m^3. The magnetic susceptibility was $\chi = 4.07 \times 10^{-8}$ m^3/kg (at 298 K). This value was corrected by Curie's law, and obtained as $\chi = 4.24 \times 10^{-8}$ m^3/kg (at 288 K) or 3.94×10^{-8} m^3/kg (at 306 K). The diameter of the enclosure is 40 mm and its height is 5.25 mm. The aspect ratio (= diameter/enclosure height) is about 7.62. Depending on the vertical level in the bore space of a superconducting magnet, the magnitudes and directions of the magnetization forces f_m differ. We defined that the center of the magnet coil was $z_b = 0$, with $z_b > 0$ upward. The direction of f_m is symmetrical with respect to the $z_b = 0$ plane. The shallow enclosure was installed at $z_b = -66$ mm in a bore space of 100-mm diameter, as shown in Figure 2. This enclosure position was selected so that the axial component of magnetization force prevails over the two other components. The experimental system is the same as that used by Maki et al.[2] and is not repeated herein.

The temperature difference between the top and bottom surfaces $\theta_h - \theta_c$ was measured by the thermocouples equipped on each of the plates. Thermal properties such as thermal diffusivity α, kinematic viscosity ν, and coefficient of volume expansion β were interpolated from the thermal data.[7] The Rayleigh numbers were computed by using the interpolated thermal properties. The magnetic field was fixed at 0–3.45 T, whereas the total heating power for a bottom plate was varied.

The relationship between the temperature differences $\theta_h - \theta_c$ and the total power supply Q is shown in Figure 3. The net heat flux and the heat loss were estimated by the method of

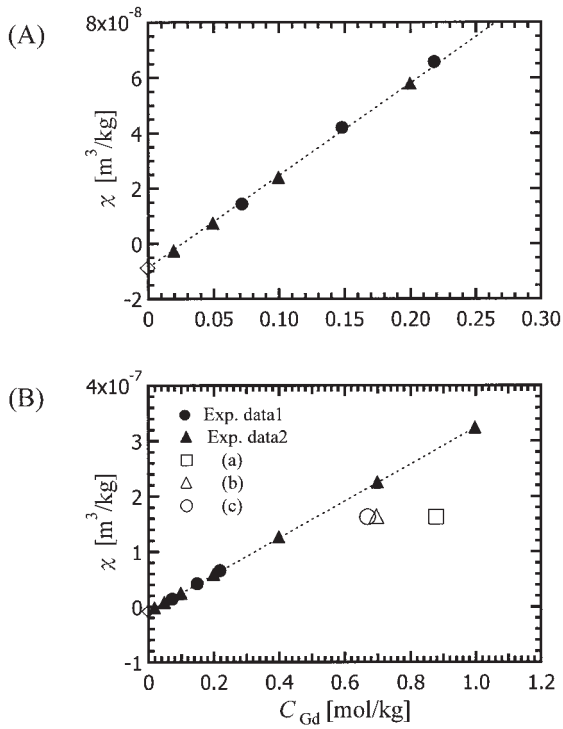

Figure 1. Relationship between the magnetic susceptibilities χ and the concentrations of gadolinium nitrate.

(A) The data in the proximity of the concentration used in our experiments. (B) The data in the whole concentration range. All of our results are converted into the values at 288 K for referring to the result by Braithwaite et al.[1] Exp. data 1 (filled circles) are the results of the first experiment, and data from Exp. data 2 (filled triangles), the second results. The open diamond in (A) represents the susceptibility of water taken from the literature. Data points (a), (b), and (c) in (B) are the values for the solution used by Braithwaite et al., assuming that the salt used was (a) anhydrate, (b) pentahydrate, and (c) hexahydrate.

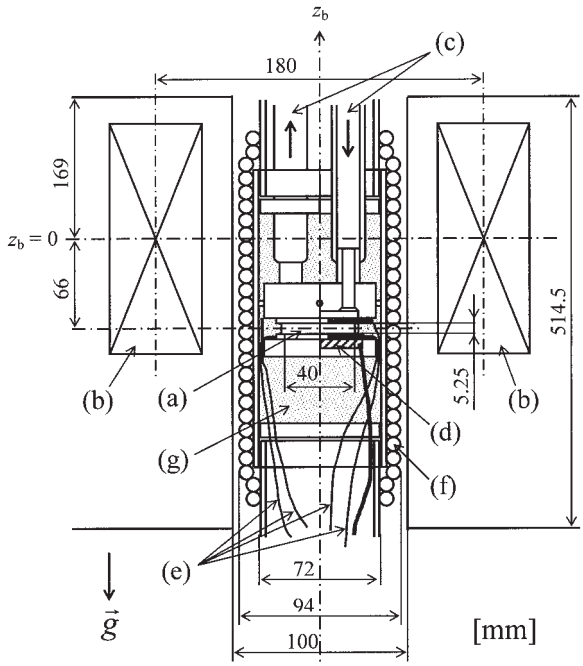

Figure 2. Perspective of the experimental apparatus with dimensions in mm.

(a) Cylindrical enclosure in the bore, (b) superconducting magnet coil, (c) circulating water to cool the top of the cylindrical enclosure, (d) heater located under the bottom of the cylindrical enclosure, (e) thermocouples, (f) rubber hose to circulate the constant temperature water, (g) heat-insulating material fully surrounding the cylindrical enclosure. The origin of z_b is also shown.

Ozoe and Churchill,[8] and the heat loss line is represented by the dot-dash line. At first, the conduction experiment was carried out with the whole experimental apparatus placed upside down, that is, heated from above and cooled from below. The net conduction heat flux through the experimental fluid layer was estimated by using Fourier's law with known thermal conductivity of the fluid, which gives the heat loss by subtracting the net conduction heat flux from the total heat supply. We can repeat this for other total heat supply to obtain the heat loss line. Then, the convection experiment was carried out with the apparatus heated from below. For the convection experiment, the net convective heat flux can be given by subtracting a heat loss from the total heat supply at the corresponding temperature difference $\theta_h - \theta_c$. For example, if a datum shown as a cross in Figure 3 is obtained, Nu is experimentally estimated as the ratio of Q_{conv} to Q_{cond}. Nu is always defined >1. When the convection is totally suppressed, Nu $= 1$.

In the absence of the magnetic field, heat transfer is attributed to usual natural convection. By progressively increasing the magnitude of upward magnetization force, the effect of gravity is decreased, and the convection becomes stagnated. As a result, the temperature difference $\theta_h - \theta_c$ increases and, finally, the conduction state is attained at the loss of acceleration force. In short, the convection almost disappears, leading to the quasi-non-gravitational state, although the liquid is heated from below.

Disappearance of convection would also have been observed simply by visual inspection of fluidal motion. However, the narrow magnet bore prevented such an experiment. Therefore, we proceeded to carry out numerical analyses to pursue the convection, observed in Figure 3.

Model Equations for the Convection of Paramagnetic Liquids

The magnetization force f_m with magnetic flux density $\vec{b} = (b_r, b_\phi, b_z)$ on a paramagnetic substance with magnetic susceptibility χ_m is as follows[1]

$$f_m = \frac{\chi_m}{2\mu_0} \vec{\nabla} b^2 \tag{1}$$

For a paramagnetic fluid, the mass magnetic susceptibility is inversely proportional to its absolute temperature by Curie's law. For the present experimental fluid, the state equation is given by the next equation with a volumetric coefficient of expansion β near the average temperature θ_0

$$\rho = \frac{\rho_0}{1 + \beta(\theta - \theta_0)} \tag{2}$$

By use of a procedure similar to the Boussinesq approximation, as was carried out by Tagawa et al.,[9] the momentum equation was obtained including both magnetization force and gravitational force. The basic equations were nondimensionalized by the way of Hellums and Churchill as follows.[10] They are equations of continuity (Eq. 3), energy balance (Eq. 4), and momentum for the paramagnetic liquid (Eq. 5), a nondimensional parameter for a paramagnetic liquid (Eq. 6), and a nondimensional parameter representing the magnitude of the

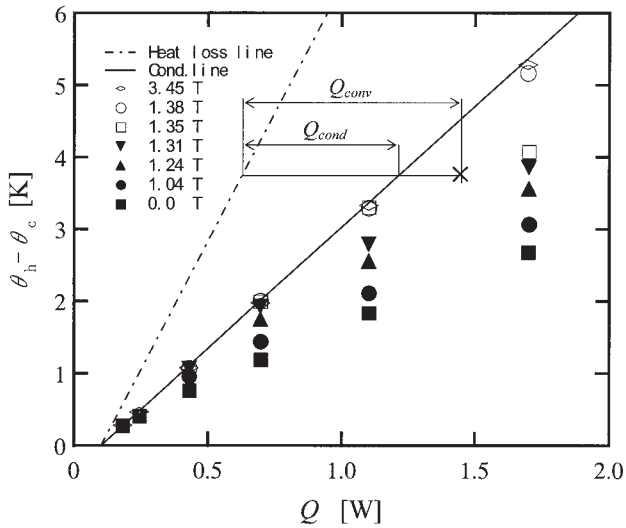

Figure 3. Experimental results representing the relation between the temperature difference $\theta_h - \theta_c$ (K) and the total electric power for heating Q (W).

The conduction line is represented as Cond. line in this figure. The net heat flux and the heat loss were estimated by the method of Ozoe and Churchill,[8] and the heat loss is represented in this figure as the Heat loss line. If a datum shown as a cross is obtained, the Nusselt number (Nu) is experimentally estimated as the ratio of Q_{conv} to Q_{cond}. The ratio is always >1, approaching 1 when convection is stagnated.

magnetization force (Eq. 7). In Eq. 4, ∇^2 means $(\nabla\cdot\nabla^t)$, where $\nabla = (\partial/\partial x, \partial/\partial y, \partial/\partial z)$.

$$\vec{\nabla}\cdot\vec{U} = 0 \tag{3}$$

$$\frac{DT}{D\tau} = \nabla^2 T \tag{4}$$

$$\frac{D\vec{U}}{D\tau} = -\vec{\nabla}P + \mathrm{Pr}\,\nabla^2\vec{U} + \mathrm{Ra}\cdot\mathrm{Pr}\cdot T\left[\begin{pmatrix}0\\0\\1\end{pmatrix} - \gamma\frac{C}{2}\vec{\nabla}(\vec{B})^2\right] \tag{5}$$

$$C = 1 + \frac{1}{\beta\theta_0} \tag{6}$$

$$\gamma = \frac{\chi_m b_a^2}{\mu_0\rho_0 g h} \tag{7}$$

We considered that the aspect ratio of the enclosure was 8.0, the top surface ($Z = +0.5$) was cold, the bottom ($Z = -0.5$) was hot, and the side wall ($R = 4.0$) was adiabatic. The initial and boundary conditions are as follows

At $\tau = 0$

$$\vec{U} = \vec{0} \qquad T = 0 \tag{8}$$

At $Z = +0.5$

$$\vec{U} = \vec{0} \qquad T = -0.5 \tag{9}$$

At $Z = -0.5$

$$\vec{U} = \vec{0} \qquad T = +0.5 \tag{10}$$

At $R = 4.0$

$$\vec{U} = \vec{0} \qquad \frac{\partial T}{\partial R} = 0 \tag{11}$$

Fully three-dimensional calculations were carried out to solve Eqs. 3–7 using a cylindrical coordinate with the HSMAC (highly simplified marker and cell) scheme for a staggered mesh system.[11] The value of Nu was computed at $Z = +0.5$ as a measure to determine the contribution of convection in reference to conduction.

Several numerical computations were carried out with various numbers of meshes for the system at Pr = 6.0, Ra = 7020, and aspect ratio = 8.0. Table 2 summarizes the results. From these results, we adopted the mesh numbers of 21 in the radial direction, 41 in the circumferential direction, and 21 in the axial direction. Figure 4 shows these grids in top and side views.

Table 2. Effect of the Grid Size on the Numerical Computation at Pr = 6.0, Ra = 7020, and without Applying the Magnetic Field

R	ϕ	Z	Nu
21	21	15	2.39
21	21	21	2.29
21	41	21	2.29
21	41	25	2.27

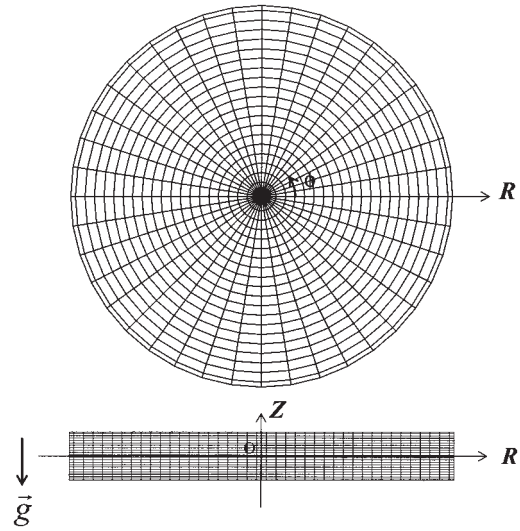

Figure 4. Top and side views of the grids for the numerical computation.

Computed Results

Sample computations were carried out at Pr = 6.0, and Ra = 7020 and 14,040. The mean temperature of the fluid was assumed to be 306 K. At this temperature and without a magnetic field, if the height of the enclosure h as a representative length is 5 mm, the temperature difference between the cold top surface and the hot bottom becomes 2.05°C at Ra = 7020 and 4.11°C at Ra = 14,040.

At first, natural convection was computed to use it as the initial condition for the magnetization convection. In the computation, the superconducting magnet as a source of the magnetization force is replaced with a one-turn coil whose diameter is $36h$. The enclosure is located at $z = -11h$, where the axial components of magnetization force are dominant.

Figure 5 shows the distributions of the magnetization force vectors in the shallow cylindrical enclosure located at various

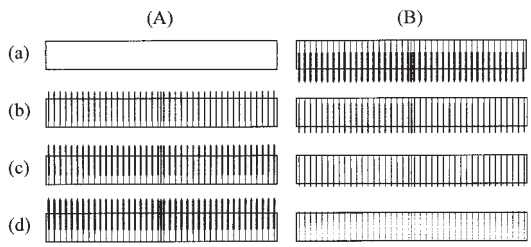

Figure 5. Force distributions in the shallow cylindrical enclosure.

(A) Magnetization force, $-\gamma(C/2)\vec{\nabla}(\vec{B})^2$, (B) the resultant forces with gravity $(0, 0, 1)^T - \gamma(C/2)\vec{\nabla}(\vec{B})^2$. The magnitude of magnetization force at the center of the enclosure $F_m^{R,Z=0}$ (nondimensional): (a) 0, (b) 0.5, (c) 0.75, and (d) 1.0.

Table 3. Summary of the Computed Results*

Ra	Ra_m	γ	$F_m^{R,Z=0}$	Nu	Max. Vel. (mm/s)	Figure Number
7020	7020	0	0	2.29	0.92	6a
	3510	2009	0.50	1.69	0.36	6b
	1755	3013	0.75	1.0005	0.02	6c
	0	4018	1.00	1.0002	0.01	6d
14,040	14040	0	0	2.62	1.10	7a
	7020	2009	0.50	2.27	0.91	7b
	3510	3013	0.75	1.63	0.36	7c
	0	4018	1.00	1.0002	0.01	7d

*These computations were carried out at Pr = 6.0, C = 11.3, and Ra = 7020 and 14,040, and the mean temperature of the fluid was assumed to be 306 K. Max. Vel. corresponds to the maximum velocity of the convection for the height of the enclosure of 5 mm.

levels. Figure 5A shows the distributions of the magnetization force $-\gamma(C/2)\vec{\nabla}(\vec{B})^2$, and Figure 5B represents the distributions of the resultant force from the magnetization force and gravity $(0, 0, 1)^T - \gamma(C/2)\vec{\nabla}(\vec{B})^2$. In other words, Figure 5B shows the distributions of the residual force in the enclosure. The magnitude of the magnetization force at the center of the enclosure $F_m^{R,Z=0}$ (in nondimensional units) is: (a) 0, (b) 0.5, (c) 0.75, or (d) 1.0.

The computed results are summarized in Table 3. The numerical isothermal distributions and the velocity distributions are shown in Figures 6 and 7. In particular, the isothermal distributions are shown both for horizontal sections at $Z = 0$ and for vertical sections at $\phi = 0$. The values of Nu in Table 3 are also included in Figure 8.

For this computation at Pr = 6.0, even the three-dimensional computation gave axially symmetric solutions, although non-axial solutions were obtained at Pr = 0.7.[2] Nu decreased gradually when the applied upward magnetization force was enhanced. At Ra values of 7020 and 14,040, quasi-non-gravitational states were achieved, as shown in Figure 6d and Figure 7d for the vanishing net acceleration cases. On the other hand,

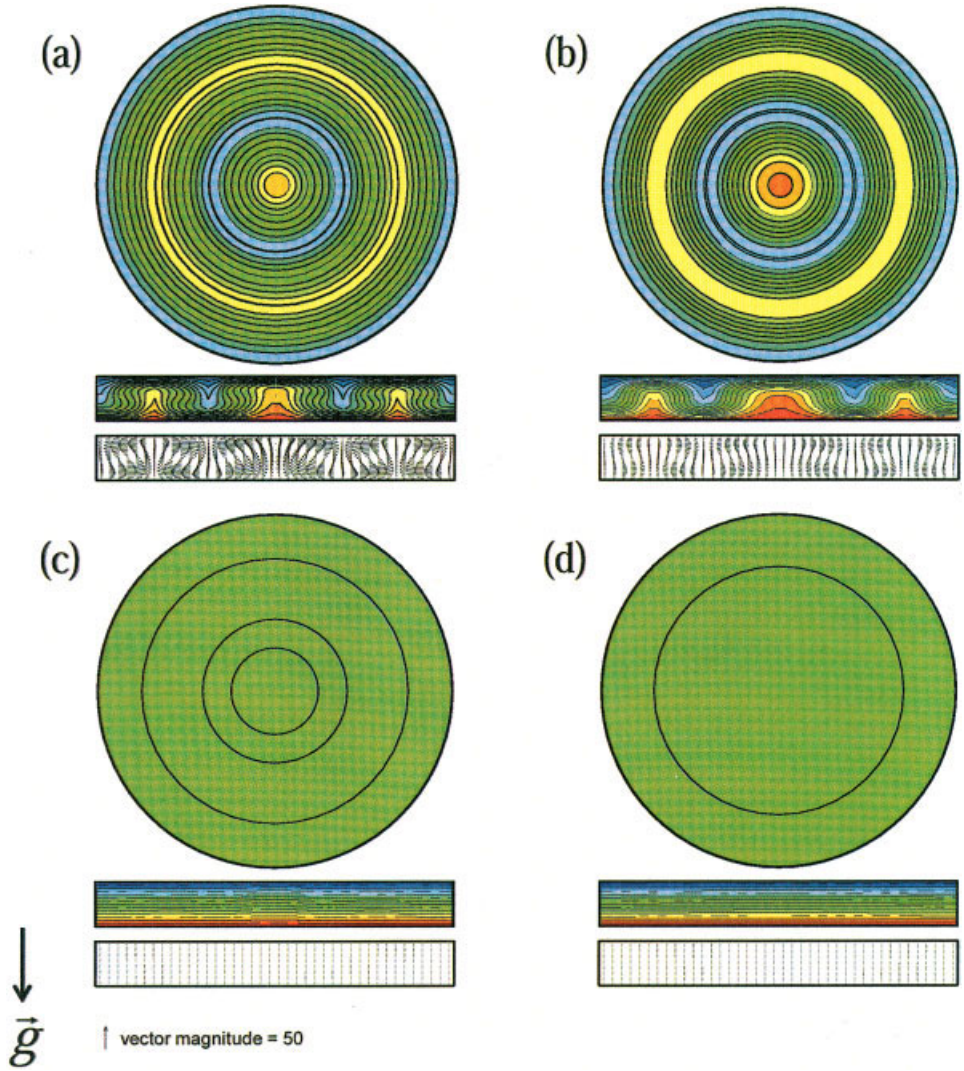

Figure 6. Computed results for the top view of isotherms at $Z = 0$, and isotherms and velocity vectors for vertical sections at $\phi = 0$.

The parameters are Pr = 6.0, C = 11.3, and Ra = 7020. The magnitude of magnetization force at the center of the enclosure $F_m^{R,Z=0}$ (nondimensional): (a) 0, (b) 0.5, (c) 0.75, and (d) 1.0.

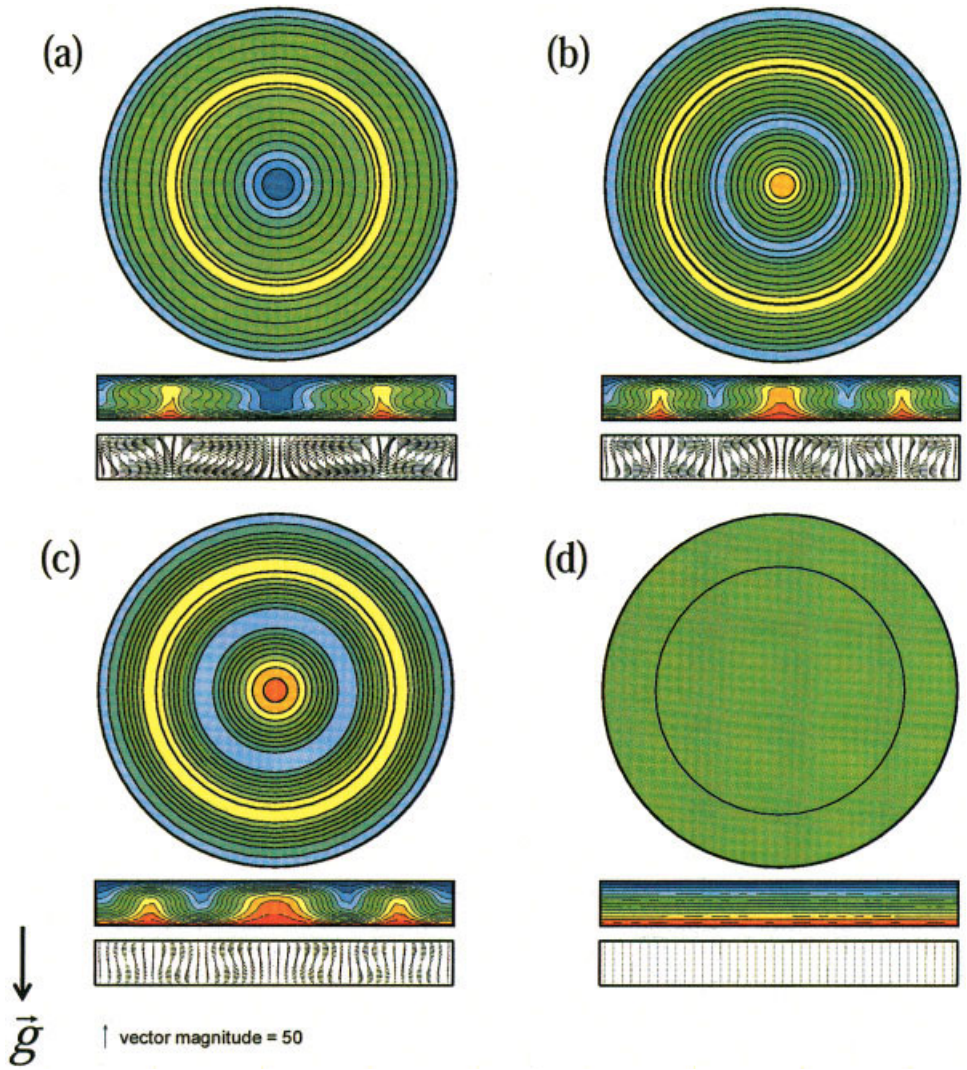

Figure 7. Computed results for the top view of isotherms at $Z = 0$, and isotherms and velocity vectors for vertical sections at $\phi = 0$.

The parameters are Pr = 6.0, C = 11.3, and Ra = 14,040. The magnitude of magnetization force at the center of the enclosure $F_m^{R,Z=0}$ (nondimensional): (a) 0, (b) 0.5, (c) 0.75, and (d) 1.0.

when some residual forces remained, as shown in Figure 5Bc, convection was achieved, as shown in Figure 7c.

Another finding was that the flow patterns were quite similar between Figure 6a and Figure 7b, and likewise between Figure 6b and Figure 7c. In these pairs, although the Ra numbers are different from each other, the Ra_m numbers are the same, and both Nu numbers and the maximum velocities are almost the same, as shown in Table 3. This means that it is possible to make the convection modes almost equal by using magnetization force for different Ra numbers.

Discussion

Figure 8A represents our experimental results as a relationship between Nu and Ra. These results seem to be quite complicated. However, by introducing Ra_m (Eq. 12), originally defined by Braithwaite et al.,[1] all the results corresponded quite well with Silveston's experimental curve, obtained without a magnetic field, as shown in Figure 8B

$$\mathrm{Ra}_m = \mathrm{Ra}\left\{1 - \frac{\chi_m}{\mu_0 \rho_0 g}\left(1 + \frac{1}{\beta\theta_0}\right) b_z \frac{\partial b_z}{\partial z}\right\} \qquad (12)$$

It is understood from Figure 8B that, when $Ra_m < 1708$, the complete suppression of convection takes place.

By the use of gadolinium nitrate, Braithwaite et al.[1] carried out the convectional experiments by using magnetization force under both convection-suppressing and convection-promoting conditions. Their experiment is recognized as the vanguard in demonstrating the quasi-non-gravitational state. The convection results by Braithwaite et al. are also shown in Figures 8A and B. Their data collected under the condition $\mu_0^2 H(dH/dz) = 0, -4.0$, and $+4.0$ are represented as (1), (2), and, (3) respectively. Their data (1) did not agree with Silveston's experimental curve in either Figure 8A or Figure 8B. In Figure 8B, their data (1) and (2) at $\mu_0^2 H(dH/dz) = 0$ and -4.0, respectively, agree with each other but not with that of Silveston. Their data

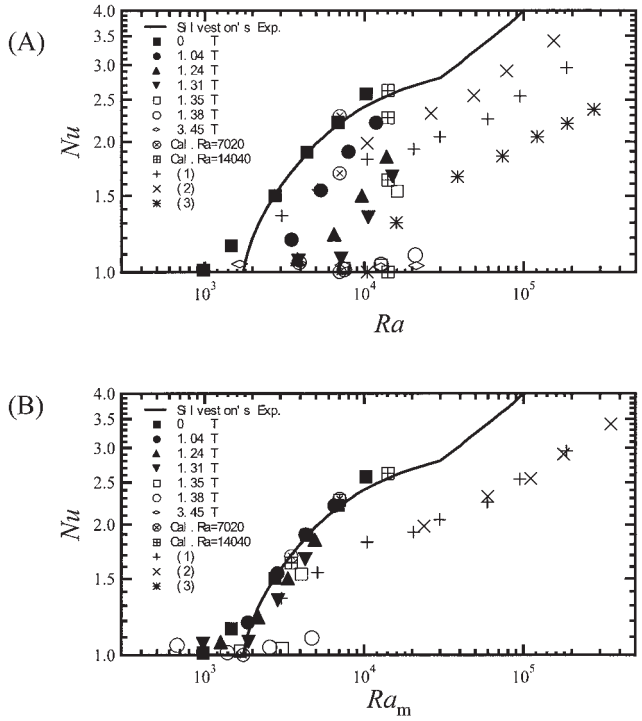

Figure 8. Measured and computed Nusselt number (A) arranged by using Ra, and (B) rearranged by Ra_m.

(1) $\mu_0^2 H(dH/dz) = 0$, (2) $\mu_0^2 H(dH/dz) = -4.0$, (3) $\mu_0^2 H(dH/dz) = +4.0$.

(3) at $\mu_0^2 H(dH/dz) = +4.0$ do not fall in the present range of Ra_m and are not shown in Figure 8B.

Our computed results, included in Figures 8A and B, corresponded well with Silveston's curve in Figure 8B, as did the above-mentioned experimental results.

In the above numerical computation with a paramagnetic liquid, we introduced in Eq. 6 the nondimensional parameter C. The joint use of γ and C is considered to help us understand the specific effects of the magnetization force on paramagnetic liquids. Ra_m in Eq. 12 can be rearranged as follows

$$\mathrm{Ra}_m = \mathrm{Ra}\left(1 - \gamma \frac{C}{2} \frac{\partial B_Z^2}{\partial Z}\right) \tag{13}$$

The parameter γ can be used generally for a paramagnetic liquid, a paramagnetic gas, and a diamagnetic fluid (gas, liquid). On the other hand, the parameter C depends only on the thermal properties, which manifest themselves only when magnetization force exists. The magnitude of C is quite large for paramagnetic liquids: it is 11.3 at 306 K, 18.1 at 293 K, and 40.2 at 283 K for our solution. Thus, because C substantially varies with temperature, quantitative convection control is difficult only by using the magnetic parameter γ. In calculating C, we used the volumetric expansion coefficient β of water because the ionic concentration is small. We think that the joint use of γ and C enables the effects of the magnetization force and the thermal properties to be considered separately. It is added that, for a paramagnetic gas such as air, $C = 2$ constantly,[2,9,12] and for diamagnetic fluids, $C = 1$ constantly.[13]

Conclusions

The magnetization convection of aqueous gadolinium nitrate solution, a typical paramagnetic liquid, was studied. Its magnetic susceptibility was measured by the Gouy method. The convection in a shallow enclosure was progressively suppressed by the upward magnetization force, and we confirmed the transition into the quasi-non-gravitational state by using the inhomogeneous magnetic field that a superconducting magnet provides.

The experimental and numerical Nusselt numbers were plotted vs. the magnetic Rayleigh number Ra_m, which fitted with Silveston's experimental curve, obtained without a magnetic field.[3] The numerical computations showed that the flow patterns became quite similar if Ra_m values were equal. Thus, it was shown that the use of Ra_m is essential to control convection.

Notation

$\vec{B}$ = nondimensionalized magnetic flux density vector = (B_r, B_ϕ, B_z)
$\vec{b}$ = magnetic flux density vector = (b_r, b_ϕ, b_z), T = Wb/m^2 = V s m^{-2}
b_a = representative magnetic flux density = $\mu_0 i/h$, T
C = nondimensional parameter for paramagnetic liquid = $1 + (1/\beta\theta_0)$
c_{Gd} = concentration of gadolinium nitrate, mol/kg
f_m = magnetization force, N/m^3
$F_m^{R,Z=0}$ = magnitude of the magnetization force at the center of the enclosure
$\vec{g}$ = gravitational vector = (0, 0, $-g$)
h = height of an enclosure, m
H = magnetic intensity, A/m
i = electric current in a coil, A
Nu = nondimensional Nusselt number = Q_{conv}/Q_{cond}
P = nondimensionalized pressure
p = pressure, N/m^2
Pr = nondimensional Prandtl number = ν/α
Q = total electric power for heating, W
Q_{conv} = heat transfer by convection, W
Q_{cond} = heat transfer by conduction, W
r = radial component fixed to the enclosure, m
R = nondimensionalized radial component fixed to the enclosure
Ra = nondimensional Rayleigh number = $g\beta\theta_h - \theta_c h^3/(\alpha\nu)$
Ra_m = magnetic Rayleigh number, = Ra$\{1 - [\gamma(C/2)(\partial B_Z^2/\partial Z)]\}$
t = time, s
T = nondimensionalized temperature
u = radial velocity component of solution, m/s
$\vec{u}$ = velocity vector = (u, v, w), m/s
$\vec{U}$ = nondimensionalized velocity vector
v = circumferential velocity component of solution, m/s
w = axial velocity component of solution, m/s
z = axial component fixed to the enclosure, m
Z = nondimensionalized axial component fixed to the enclosure
z_b = axial component whose origin is at the center of the magnet, m

Greek letters

α = thermal diffusivity of solution, m^2/s
β = volumetric coefficient of expansion of fluid resulting from temperature difference, 1/K
γ = nondimensional parameter representing the magnitude of the magnetization force = $\chi_m b_a^2/(\mu_0\rho_0 g h)$
θ = temperature, K
θ_h = hot surface temperature, K
θ_c = cold surface temperature, K

θ_o = representative temperature = $(\theta_h + \theta_c)/2$, K
μ_0 = magnetic permeability, H/m
ν = kinematic viscosity, m^2/s
ρ = density of solution, kg/m^3
ρ_0 = density of solution at θ_0, kg/m^3
ρ_{sol} = density of aqueous gadolinium nitrate solution, kg/m^3
τ = nondimensionalized time
ϕ = circumferential angle coordinate fixed to the enclosure, rad
χ = magnetic susceptibility of solution, m^3/kg
χ_m = nondimensional magnetic susceptibility of solution, $\chi_m = \rho\chi$

Literature Cited

1. Braithwaite D, Beaugnon E, Tournier R. Magnetically controlled convection in a paramagnetic fluid. *Nature.* 1991;354:134-135.
2. Maki S, Tagawa T, Ozoe H. Enhanced convection or quasi-conduction states measured in a super-conducting magnet for air in a vertical cylindrical enclosure heated from below and cooled from above in a gravity field. *J Heat Transfer.* 2002;124:667-673.
3. Chandrasekhar C. *Hydrodynamic and Hydromagnetic Stability*. Dover, UK: Oxford Univ. Press, 1961:68.
4. Maki S, Oda Y, Ataka M. High-quality crystallization of lysozyme by magneto-Archimedes levitation in a superconducting magnet. *J Cryst Growth.* 2004;261:557-565.
5. Ikezoe Y, Hirota N, Nakagawa J, Kitazawa K. Making water levitate. *Nature.* 1998;393:749-750.
6. Yamato M, Nakazawa H, Kimura T. Levitation polymerization to fabricate a large polymer sphere. *Langmuir.* 2002;18:9609-9610.
7. Holman JP. *Heat Transfer*. 7th ed. (in SI Units). London: McGraw-Hill, 1992:663.
8. Ozoe H, Churchill SW. Hydrodynamic stability and natural convection in Newtonian and non-Newtonian fluids heated from below. *AIChE Symp Ser, Heat Transfer.* 1973;69:126-133.
9. Tagawa T, Shigemitsu R, Ozoe H. Magnetizing force modeled and numerically solved for natural convection of air in a cubic enclosure: Effect of the direction of the magnetic field. *Int J Heat Mass Transfer.* 2002;45:267-277.
10. Hellums JD, Churchill SW. Simplification of the mathematical description of boundary and initial value problems. *AIChE J.* 1964;10:110-114.
11. Hirt CW, Nichols BD, Romero NC. A numerical solution algorithm for transient fluid flows. Los Alamos, NM: Los Alamos National Laboratory, LA-5852; 1975.
12. Maki S, Tagawa T, Ozoe H. Average heat transfer rates measured and numerically analyzed for combined convection of air in an inclined cylindrical enclosure due to both magnetic and gravitational fields. *Exp Therm Fluid Sci*. 2003;27:891-899.
13. Tagawa T, Ujihara A, Ozoe H. Numerical computation for Rayleigh–Benard convection of water in a magnetic field. *Int J Heat Mass Transfer.* 2003;46:4097-4104.

Manuscript received Feb. 19, 2004, revision received July 21, 2004, and final revision received Dec. 14, 2004.